Quantitative Parameter Mapping of Contrast Agent Concentration and Relaxivity and Brain Tumor Extracellular pH

Yuki Matsumoto (lakaisbmtyk@gmail.com)
Tokushima University
Masafumi Harada
Tokushima University
Yuki Kanazawa
Tokushima University
Yo Taniguchi
FUJIFILM Healthcare Corporation
Masaharu Ono
FUJIFILM Healthcare Corporation
Bito Yoshitaka
FUJIFILM Healthcare Corporation

Research Article

Keywords: magnetic resonance imaging (MRI), brain tumors, longitudinal relaxivity (r1), pathophysiological tumor

Posted Date: July 26th, 2021

DOI: https://doi.org/10.21203/rs.3.rs-726378/v1

Version of Record: A version of this preprint was published at Scientific Reports on February 9th, 2022.
See the published version at https://doi.org/10.1038/s41598-022-05711-z.

Quantitative parameter mapping of contrast agent concentration and relaxivity and brain tumor extracellular pH

Yuki Matsumoto[1*], Masafumi Harada[1], Yuki Kanazawa[1], Yo Taniguchi[2], Masaharu Ono[2], Bito Yoshitaka[2]

[1] Tokushima University, Graduate School of Biomedical Sciences, Tokushima city, 770-8503, Japan

[2] FUJIFILM Healthcare Corporation, Tokyo, 110-0015, Japan

*lakaisbmtyk@gmail.com

Abstract

In clinical magnetic resonance imaging (MRI), gadolinium-based contrast agents are most commonly used for evaluating brain tumors. However, contrast-enhanced MRI can only provide relative signal changes such as mixed information with longitudinal relaxivity (r1) and contrast agent concentration. Herein, we present a new method to evaluate r1 and contrast agent concentration separately in contrast-enhanced lesions using quantitative parameter mapping. We demonstrated that it is possible to evaluate pathophysiological tumor changes owing to therapeutic efficacy. Furthermore, the r1 value can be used as an extracellular pH tumor marker. We believe that our method has an easy clinical application and demonstrates how acidic environments affect the T1 relaxation time of contrast agents. In conclusion, these indices can be useful for brain tumor management.

Introduction

The effect of contrast enhancement by a gadolinium (Gd)-based contrast agent (CA) depends on both its concentration and longitudinal relaxivity (r1) in lesions. It is well known that the r1 of a Gd-based CA is affected by the rate of exchange interaction of water protons, which is influenced by factors around the lesion area, such as pH, temperature, and diffusivity [1-3]. Therefore, the r1 of a CA may reflect the biological environment of the lesion and act as an index of the lesion microenvironment. The pharmacokinetic parameter of Gd-based CAs is spin-lattice relaxation time constant (T_1)-shortening because of leakage to extracellular tissues from cerebral vessels owing to blood-brain barrier destruction, which allows the CA to leak out into the extracellular space [4]. The mechanism of the shortened-T1 is mainly due to dipole-dipole interactions of coordinated water molecule with the Gd3+ complex [5,6]. Furthermore, the acidic environment caused by anabolic metabolism in the extracellular space can act as a physical source for rotational changes of the Gd3+.

The concentration of CA and CA's r1 should be independently measured because CA concentration in a lesion depends on several factors including pathophysiological conditions. Quantitative parameter mapping (QPM) is a recently proposed method among synthetic magnetic resonance imaging (MRI) techniques [7]; it uses three dimensional (3D) spoiled gradient-echo pulse sequences with multiple repetition times, echo times, and flip angle values, thereby allowing quantitative measurement of relaxation times, proton density, and susceptibility distribution. One of the important advantages of QPM is that both relaxation and quantitative susceptibility mapping (QSM) can be independently obtained. We considered that QPM before and after CA injection would allow the separate quantification of both r1 and CA concentration using two parameters

derived from subtracted longitudinal relaxation rate (R1) and QSMs.

Several studies have shown the dependency of Gd-based CA pharmacokinetics on pH [8-11]. Although it is possible to assess pH changes by measuring relaxation rates, few studies have demonstrated the relationship between relaxation rate and pH of commercially available Gd-based CAs.

This study aimed to separately assess the effect of CA's r1 value and concentration to evaluate the possibility of a new index for r1 and measure extracellular pH (pHe) values to obtain pathophysiological information on brain tumors. Therefore, we performed a phantom experiment to investigate the r1 value of a commercially available Gd-based CA, Gd-BTDO3A, and evaluated the relationship between r1 and pH to develop a pH calibration curve at each r1 value in Gd-BTDO3A using a non-linear function, as previously reported [9].

Methods

Subjects and data acquisition

All clinical investigations were conducted according to the principles expressed in the Declaration of Helsinki. To verify that the pHe map can be measured both before and after CA injection, nine brain tumor patients (radiation necrosis: three lesions in three patients, brain metastasis: 12 lesions in four patients, primary brain tumor: two lesions in two patients), all of whom provided informed consent, underwent MRI (Table 1). This study was approved by our institutional review board (Tokushima University Hospital), and all MRI data acquired using a 3-T system (FUJIFILM Healthcare Corporation, Japan) with a 32-element-phased array receive coil. QPM employs 3D partially radio frequency (RF)-spoiled steady state gradient-echo (3D-pRSSG) methods with multiple repetition

time, echo-time, and flip angle values. To achieve adequate T1 and T2 relaxation times, imaging parameters are optimized using the law of error propagation with target relaxation times at 3T [11]. In addition, the first RF excitations (up to 50 cycles) were skipped to reach steady state. Imaging parameters were as follows: echo times, 4.5–36.8 ms; repetition times, 10–41.3 ms; and flip angles, 10–40 degrees. Image resolution was 0.94 × 0.94 × 2 mm with a 240 × 240 mm^2 FOV. Parallel imaging was used to reduce overall scan time, and the acceleration factor was 1.9 × 1.9 (RL × AP). CA amounted to 0.1 mmol/kg of body weight and was injected into the patient's vascular system. Whole-brain acquisition was then performed using the same imaging parameters as pre-injection. Note that the whole brain was scanned ≥1 min after CA injection.

Phantom experiment for pH calibration

r1 is generally defined as the slope of the resulting fit from a linear regression of the measured R1 (i.e., 1/T1) of the tissue and CA concentration [12,13] as follows:

$$\boldsymbol{R1_{post} = R1_{pre} + r1 \times CA} \quad \text{Eq. 1a}$$

$$\boldsymbol{\therefore r1 = \frac{R1_{post} - R1_{pre}}{CA}} \quad \text{Eq. 1b}$$

where $R1_{pre}$ and $R1_{post}$ denote the R1 values of the tissue before and after CA injection, respectively. CA denotes the CA concentration. The relaxivity r1 can thus be estimated by measuring $R1_{pre}$, $R1_{post}$, and CA, as shown in Eq. 1b. Here, the measured relaxivity value is different in acid pH; thus, the empirical relationship between those values must be investigated to calculate the pHe. To validate r1 depending on the pHe, a phantom experiment was then performed using a pH buffer solution, and r1 at each pH acidity was measured. We prepared various pH solution samples of known acidity (pH range of 6.0–

7.8), including the CA Gd-BTDO3A (Gadovist, Bayer HealthCare) at different concentrations (0.1, 0.2, and 0.4 mmol). The pH of these samples was achieved by mixing sodium dihydrogenphosphate dihydrate (0.2 mmol) and di-sodium hydrogen phosphate 7-hydrate (0.2 mmol) solutions. Additionally, real pH solutions were measured with a calibrated HI 2020-01 pH meter (HANNA instruments, USA). Then, the sample containers were placed in the MR exam table so that the axes of the sample containers were perpendicular to the main field, and a 3T MRI system (FUJIFILM Healthcare Corporation, Japan) used at room temperature. To measure the T1, a single slice of a coronal scan was obtained using a fast spin-echo based inversion recovery (FSE-IR) with the following parameters. Inversion time (TI) was performed at 40, 60, 70, 100, 140, 160, 200, 250,300, 600, 800, 1000, 1500, 1700, and 2000 ms. Then, the selected constant value depending on the TI was chosen so that TR = TI + 18000 ms. The shortest possible effective echo-time value (eTEs) was used: 22.2 ms. The other imaging parameters were as follows: field of view (FOV), 288 mm; imaging matrices and reconstruction matrices, 288×288 mm^2; and slice thickness, 5 mm.

Determination of the pH-relaxivity curve

Here, we describe how the pH-relaxivity calibration curve can be calculated from T1 maps. Non-linear least square fitting was first performed to yield longitudinal relaxation times T1 using the following equation:

$$S_{TI} = abs\left[M0 \times (1 - 2 \times \exp(\frac{-TI}{T1}))\right], \qquad \text{Eq. 2}$$

Where SI defines the MR signal, and the subscript TI refers to each variable obtained at TI. M0 and T1 define equilibrium magnetization and longitudinal relaxation times, respectively. The mean R1 value of each container was determined by drawing a region-

of-interest (ROI), which was an equally sized round shape (321 pixels). After a linear regression analysis based on Eq. 1b was performed, r1 values were individually calculated at each pH. In this study, the pH-sensitive range was chosen as previously reported [14] because it exhibits unique characteristics depending on the CA's chemical structure. The pH can then be calculated using least square fitting of Hill-modified Henderson-Hasselbach equation:

$$pH = pKa - log_{10}\left[\frac{r1-r1_{base}}{r1_{acid}-r1}\right]^{n} \quad \text{Eq. 3}$$

where r1 defines relaxivity, and pKa, $r1_{base}$, $r1_{acid}$, and n must be determined according to r1.

Calculation of relaxivity values

An overview of data processing is provided in Fig. 1. There are several processing steps to estimate r1 before and after CA injection of the contrast agent. First, R1 and susceptibility maps were calculated from both QPM datasets before and after CA injection. The subtraction ($R_{1substraction}$) map and the CA concentration map (CA_{qsm}) were then calculated as follows:

$$R1_{subtraction} = R1_{post} - R1_{pre}, \quad \text{Eq. 4}$$

$$CA_{qsm} = \frac{\chi_{post}-\chi_{pre}}{\chi_{gd}} \times Mol_{Gd}, \quad \text{Eq. 5}$$

where χ_{pre} and χ_{post} define susceptibility values before and after CA injection, respectively, and χ_{Gd} defines CA's molar susceptibility. In addition, Mol_{Gd} defines a CA's molar concentration. In this study, multiple dipole-inversion combination with k-space segmentation (MUDICK) and 326 ppm was used for estimating χ_{pre}, χ_{post} and χ_{Gd}, respectively [15,16]. The relaxivity r_1 was subsequently estimated with Eq. 1b by

measuring $R_{1\ subtraction}$ and CA_{QSM}. Here, a linear regression analysis was performed to confirm linearity between the CA_{qsm} and the $R_{1subtraction}$ in the brain tumor. To remove division artifacts, a 3D median filter and Gaussian filter (standard deviation of 1) were applied to r_1. Finally, the pHe map was calculated based on the resulting r_1 map and the non-linear function derived from the phantom experiment.

Statistical analysis

After administering the contrast, ROIs were drawn on the R1 map and applied to the quantitative maps of $R1_{\ subtraction}$, CA_{qsm}, r1 and pHe. As the mean pH difference based on tumor malignancy would indicate the clinical potential of brain tumor pHe, a one-way analysis of variance (ANOVA) test was used to observe whether changes in the mean pHe and r1 were dependent on malignancy.

Results

Phantom experiment

Figure 2 shows r1 depending on a wide pH range. After confirming the relaxivity behavior, the pH calibration curve was defined as a pH-sensitive range. In this study, a range of 6.8–7.4 was considered as a pH-sensitive range, and a non-linear regression analysis performed. The fitted result led to the following values: kPa = 6.80, $r1_{base}$ = 3.90, and $r1_{acid}$ = 5.5 n = 1.25.

Brain tumor

The comparison between CA_{QSM} and $R_{1\ subtraction}$ maps of all brain diseases are shown in Figure 3, demonstrating a strong correlation ($R^2 \geq 0.55$). In this study, the relationship

between CA_{QSM} and $R_{1\ subtraction}$ was individually plotted because of the mean relaxivity value, defined as the slope of the resulting fit from the linear regression. The mean brain tumor r1 changed with the anabolic metabolism in the extracellular space, indicating that CA's r1 can be independently measured by $R1_{\ subtraction}$ and CA_{qsm}. The mean values of $R_{1\ subtraction}$, CA_{QSM}, relaxivity, and pHe are shown in Figure 4.

The primary brain tumor group showed significantly higher mean r1 values than other brain disease groups ($P<0.001$). Moreover, the mean r1 of the metastasis group was significantly increased compared with radiation necrosis ($P<0.0001$). The mean pHe value showed a trend for tumor malignancy having a lower pHe value and primary brain tumor having a significantly lower pHe than other brain diseases ($P<0.001$). Moreover, the mean pHe value of the metastasis group was significantly decreased compared with the radiation necrosis one, indicating that pHe can help evaluate therapeutic efficacy ($P<0.001$). Moreover, the synthetic T_1w post contrast administration derived from QPM and pHe maps is shown in Figure 5.

Discussion

r1-based CAs have an important potential application in pHe measurement. In the early days, the r1 values were reported to show an increasing/decreasing behavior depending on the pH [14]. This behavior is that the acidic environment enhances the Gd3+ complex binding with water molecules, and therefore acidic environment plays a role in the pharmacokinetic behavior of Gd-based CA [13,20,21]. We first performed a phantom study to determine the pH sensitivity of a conventional CA, Gd-BTDO3A. In this experiment, a range of 6.8–7.4 was considered as the pH-sensitive range for the

calibration curve, resulting in four parameters: kPa = 6.80, r1base = 3.90, r1acid = 5.5, and n = 1.25.

In our approach to separately quantify CA concentration and r1, we used QPM because it can simultaneously measure the quantitative maps of both relaxation and susceptibility, leading to a clinically feasible acquisition time. We then measured QPM in patients before and after administering Gd-BTDO3A and separately quantified the CA concentration and r1 from $R_{1\mathrm{subtraction}}$ and $\mathrm{CA}_{\mathrm{QSM}}$ maps. Both maps had a high correlation with each brain disease.

An additional advantage of QPM is that standard T_1w, T_2w, T_2*w, fluid-attenuated inversion recovery images can be simultaneously obtained both before and after CA injection, which allowed adequate diagnosis of lesions, as shown in Figure 6.

A pHe map was then obtained by applying the result of the phantom experiment to the r1 map, showing that the mean pHe value decreased in the tumor grade group, as shown in Figure 4. This observation is consistent with that of earlier studies showing that the average pHe reaches approximately 6.5–7.0 in solid tumors because of the Warburg effect [22-24]. Therefore, our study proposes a new method using QPM to evaluate r1 and CA concentration in contrast-enhanced lesions, showing the possibility of evaluating tumors' pathophysiological changes. Furthermore, r1 values may be used as pHe markers. These indices may be useful for brain tumor management.

A major limitation of the conventional CA based pHe measurement is that sensitivity to CA is limited in a narrow pH range and in clinical measurements. In future work, a newly developed pH-sensitive contrast agent may be required to increase the range and accuracy of pH sensitivity. However, we believe our results to be acceptable because the mean pHe value significantly decreased in subjects with primary tumors

compared to that in those with radiation necrosis.

Our pHe measurement is specifically designed for the acidic extracellular space of solid tumors. However, our method is not restricted to brain tissue computation and can be adapted to other tissues as data acquisition is based on 3D spoiled gradient echo pulse sequences. Therefore, our methods could assist in the future application of pHe mapping to other tissues.

In conclusion, we demonstrated that it is possible to separately quantify r1 and CA concentration in brain tumors and suggested that both r1 and the calculated pHe may be a new index to manage patients with brain tumors.

Data Availability Statement

The authors confirm that the data supporting the findings of this study are available within the article.

References

[1] Reichenbach, J. *et al*. 1H T1 and T2 measurements of the MR imaging contrast agents Gd-DTPA and Gd-DTPA BMA at 1.5T. *Eur. Radiol.* **7**, 264-274 (1997).

[2] Mikawa, M., Miwa, N., Bräutigam, M., Akaike, T. & Maruyama, A. Gd3+-loaded polyion complex for pH depiction with magnetic resonance imaging. *J. Biomed. Mater. Res.* **49**, 390-395 (2000).

[3] Gerweck, L. The pH difference between tumor and normal tissue offers a tumor specific target for the treatment of cancer. *Drug Res. Updat.* **3**, 49-50 (2000).

[4] Lin, S. & Brown, J. MR contrast agents: Physical and pharmacologic basics. *J. Magn. Reson. Imaging*. **25**, 884-899 (2007).

[5] Vibhute, S. *et al.* Synthesis and characterization of pH-sensitive, biotinylated MRI contrast agents and their conjugates with avidin. *Org. Biomol. Chem.* **11**, 1294-1305 (2013).

[6] Verwilst, P., Park, S., Yoon, B. & Kim, J. Recent advances in Gd-chelate based bimodal optical/MRI contrast agents. *Chem. Soc. Rev* **44**, 1791-1806 (2015).

[7] Taniguchi, Y. *et al.* Fast 3D Multi-Parameter Mapping of Relaxation Times and Susceptibility Using Partially RF-Spoiled Gradient Echo at 3T. *ISMRM proceedings* No. 5630.

[8] Garcia-Martin, M. *et al.* High resolution pHe imaging of rat glioma using pH-dependent relaxivity. *Magn. Reson. Med.* **55**, 309-315 (2006).

[9] Martinez, G. *et al*. Imaging the extracellular pH of tumors by MRI after injection of a single cocktail of T1 and T2contrast agents. *NMR Biomed.* **24**, 1380-1391 (2011).

[10] Laus, S., Sour, A., Ruloff, R., Tóth, É. & Merbach, A. Rotational Dynamics Account for pH-Dependent Relaxivities of PAMAM Dendrimeric, Gd-Based Potential MRI Contrast Agents. *Chemistry* **11**, 3064-3076 (2005).

[11] Aime, S., Fedeli, F., Sanino, A. & Terreno, E. A R2/R1Ratiometric Procedure for a Concentration-Independent, pH-Responsive, Gd(III)-Based MRI Agent. *J. Am. Chem. Soc.* **128**, 11326-11327 (2006).

[12] Stack, J., Redmond, O., Codd, M., Dervan, P. & Ennis, J. Breast disease: tissue characterization with Gd-DTPA enhancement profiles. *Radiology* **174**, 491-494 (1990).

[13] Rohrer, M., Bauer, H., Mintorovitch, J., Requardt, M. & Weinmann, H. Comparison of Magnetic Properties of MRI Contrast Media Solutions at Different Magnetic Field Strengths. *Invest. Radiol.* **40**, 715-724 (2005).

[14] Zhang, S., Wu, K. & Sherry, A. A Novel pH-Sensitive MRI Contrast Agent. *Angew. Chem. Int. Ed. Eng.l* **38**, 3192-3194 (1999).

[15] Sato, R. et al. Quantitative Susceptibility Mapping Using the Multiple Dipole-inversion Combination with k-space Segmentation Method. *Magn. Reson. Med. Sci.* **16**, 340-350 (2017).

[16] de Rochefort, L., Brown, R., Prince, M. & Wang, Y. Quantitative MR susceptibility mapping using piece-wise constant regularized inversion of the magnetic field. *Magn. Reson. Med.* **60**, 1003-1009 (2008).

[17] Zhou, J., Payen, J., Wilson, D., Traystman, R. & van Zijl, P. Using the amide proton signals of intracellular proteins and peptides to detect pH effects in MRI. *Nat. Med.* **9**, 1085-1090 (2003).

[18] Sun, P. & Sorensen, A. Imaging pH using the chemical exchange saturation transfer (CEST) MRI: Correction of concomitant RF irradiation effects to quantify CEST MRI for chemical exchange rate and pH. *Magn. Reson. Med.* **60**, 390-397 (2008).

[19] Moon, B. *et al.* A comparison of iopromide and iopamidol, two acidoCEST MRI contrast media that measure tumor extracellular pH. *Contrast Media Mol. Imaging.* **10**, 446-455 (2015).

[20] Reuben, J. Gadolinium(III) as a paramagnetic probe for proton relaxation studies of biological macromolecules. Binding to bovine serum albumin. *Biochemistry* **10**, 2834-2838 (1971).

[21] Stanisz, G. & Henkelman, R. Gd-DTPA relaxivity depends on macromolecular content. *Magn. Reson. Med.* **44**, 665-667 (2000).

[22] Helmlinger, G., Yuan, F., Dellian, M. & Jain, R. Interstitial pH and pO2 gradients in solid tumors in vivo: High-resolution measurements reveal a lack of correlation. *Nat. Med.* **3**, 177-182 (1997).

[23] Warburg, O., Wind, F. & Negelein, E. THE METABOLISM OF TUMORS IN THE BODY. *J. Gen. Physiol.* **8**, 519-530 (1927).

[24] Gillies, R. & Gatenby, R. Hypoxia and adaptive landscapes in the evolution of carcinogenesis. *Cancer and Metastasis Rev.* **26**, 311-317 (2007).

Acknowledgements

This work was supported by JSPS KAKENHI Grant Number JP20K16759.

Author contributions (names must be given as initials)

Author contributions here are given by referring Contributor Roles Taxonomy (CRediT).

Y.M: Conceptualization, Data curation, Formal analysis, Funding acquisition, Investigation, Software, Visualization, Writing-Original Draft

M.H: Conceptualization, Funding acquisition, Investigation, Supervision, Project administration, Writing-Review & Editing

Y.K: Supervision, Writing-Review & Editing

Y.T: Software, Resources

M.O: Software, Resources

B.Y: Software, Resources

Competing interest

Y.M: This work was supported by JSPS KAKENHI Grant Number JP20K16759.

M.H: He has been funded by FUJIFILM Healthcare Corporation.

Y.K: He declares no potential conflict of interest

Y.T: Employees of the FUJIFILM Healthcare Corporation, Japan and the authors have conflict of interest to disclose with respect to this study.

M.O: Employees of the FUJIFILM Healthcare Corporation, Japan and the authors have conflict of interest to disclose with respect to this study.

B.Y: Employees of the FUJIFILM Healthcare Corporation, Japan and the authors have

conflict of interest to disclose with respect to this study.

Figure legends

Figure 1: Scheme of the procedure for pHe calculation.

Figure 2: pHe-relaxivity calibration curve.

Figure 3: Relationship between $R_{1subtraction}$ and CA_{QSM} for each brain disease.

Figure 4: Mean values of $R_{1subtraction}$, CA_{QSM}, relaxivity, and pHe.

Figure 5: Contrast-enhanced synthetic T_1w image-derived QPM and pHe maps.

Figure 6: Brain disease evaluation using QPM before and after contrast agent injection.

Table 1. Patient data

Age (years)	Sex	Clinical diagnosis	Group
79	F	Radiation necrosis #1	Radiation necrosis
61	F	Radiation necrosis #2	Radiation necrosis
72	F	Radiation necrosis #3	Radiation necrosis
68	M	Metastasis #1	Metastasis
72	F	Metastasis #2	Metastasis
74	M	Metastasis #3	Metastasis
47	F	Metastasis #4	Metastasis
49	F	Anaplastic astrocytoma	Primary brain tumor
76	F	Glioblastoma	Primary brain tumor

Figures

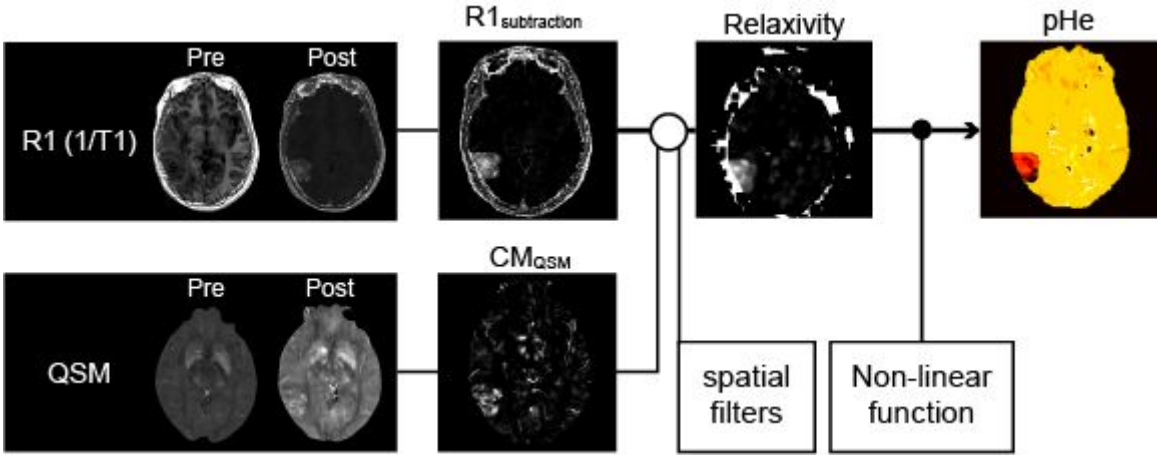

Figure 1

Scheme of the procedure for pHe calculation.

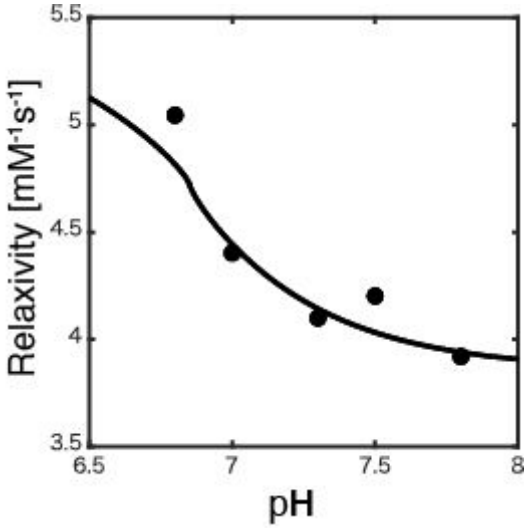

Figure 2

pHe-relaxivity calibration curve.

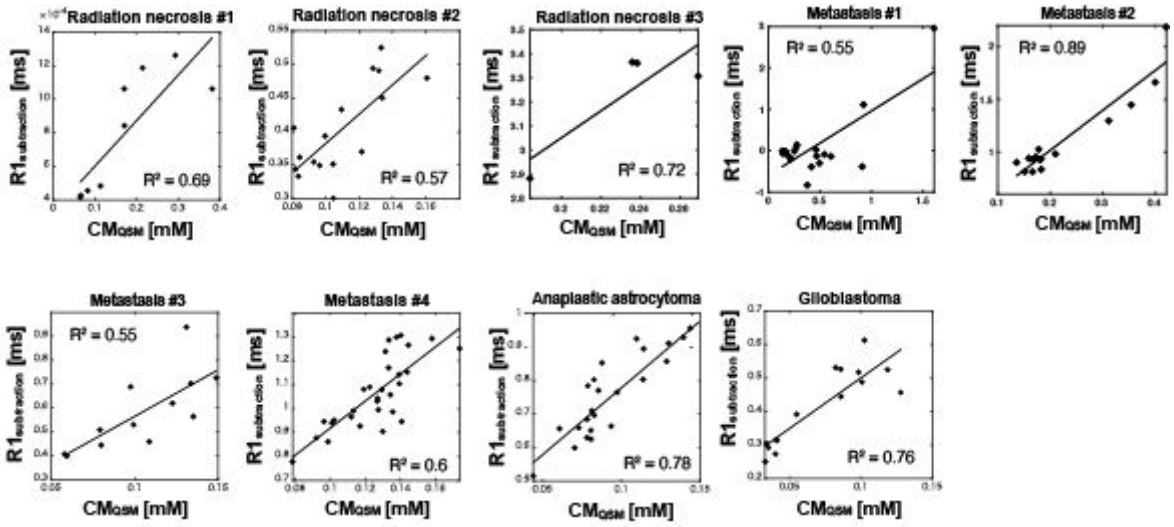

Figure 3

Relationship between R1subtraction and CAQSM for each brain disease.

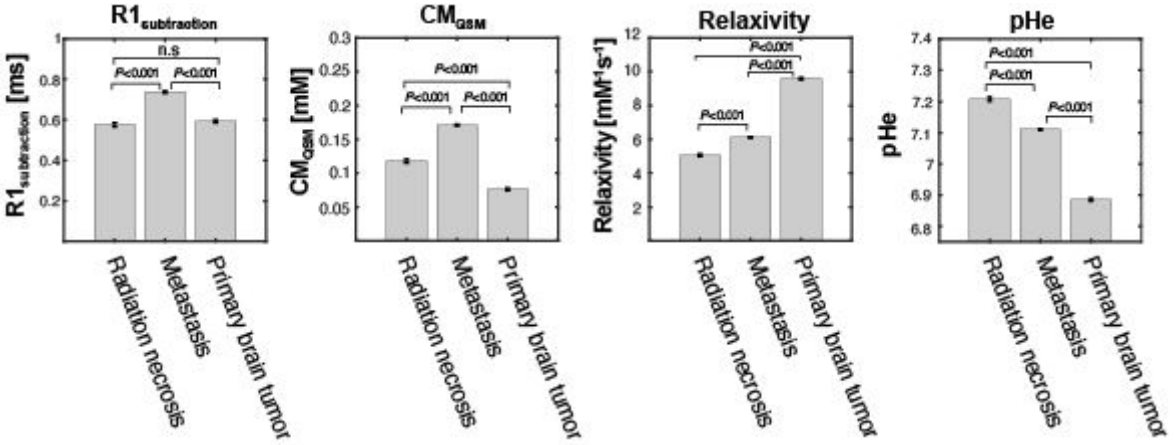

Figure 4

Mean values of R1subtraction, CAQSM, relaxivity, and pHe.

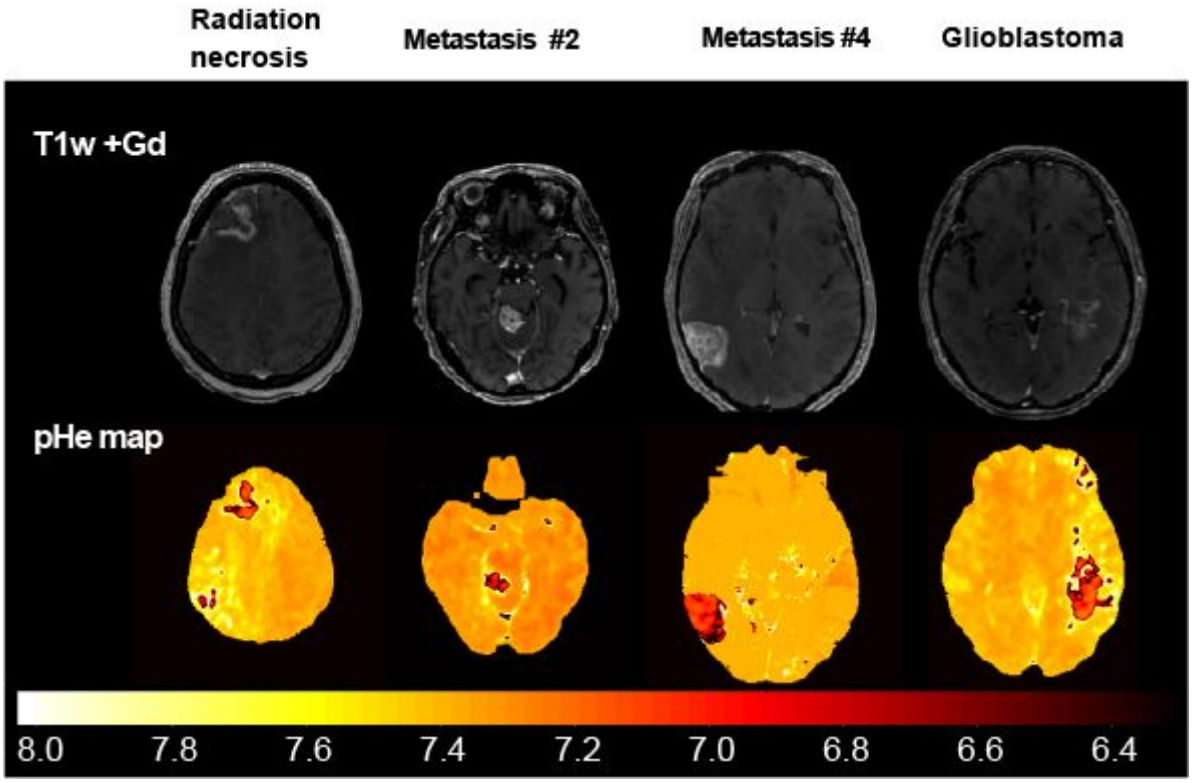

Figure 5

Contrast-enhanced synthetic T1w image-derived QPM and pHe maps.

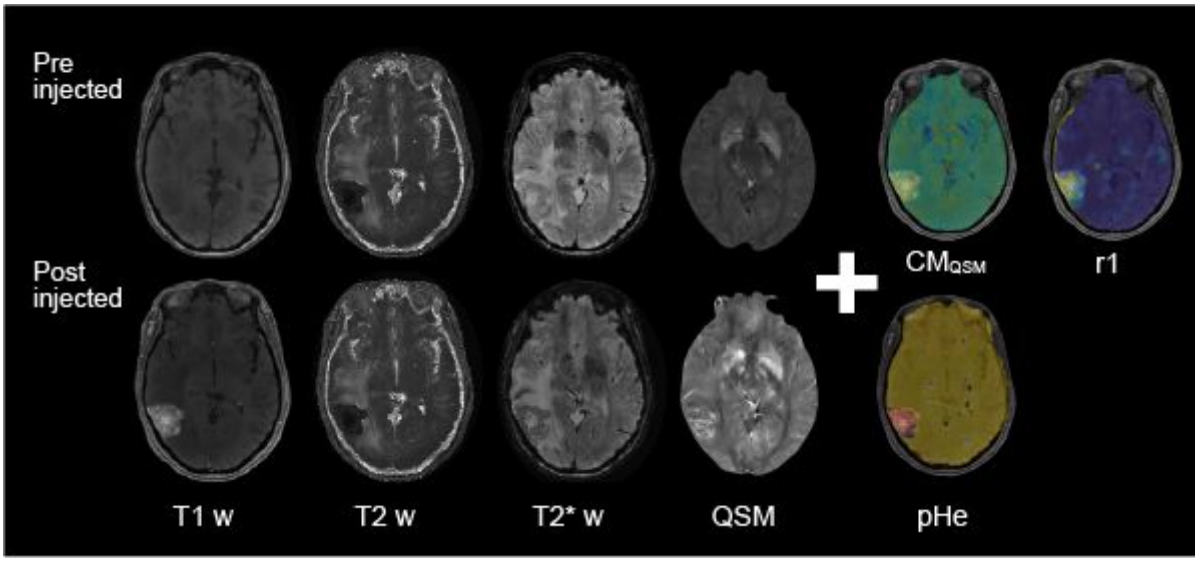

Figure 6

Brain disease evaluation using QPM before and after contrast agent injection.